

Modified Titania Films for Photoelectrochemical Applications

Shenghong Qiu and Thomas L. Starr

Department of Chemical Engineering, University of Louisville, Louisville, KY, 40207

Introduction

TiO₂ is recognized as a photocatalytic material and has been widely used because of its high functionality, long-term stability and non-toxicity. [1] However, because the band gap of pure TiO₂ for anatase crystalline phase is as high as 3.2 eV, TiO₂ shows only high reactivity under ultraviolet light. In order to make the better use with ideal energy source, sunlight, people have tried several modification of TiO₂, such as cation, anion doping and oxygen deficient. [2-4] Transition metal ion doping is one approach for acquiring a visible response by introducing defects into the lattice. [5-7] It is known that the photocatalytic activity of doped TiO₂ is determined by the methods of doping, the amount and distribution of dopants.

Incipient wet impregnation and coprecipitation methods are mostly used to produce metal doped TiO₂ in the literatures. However, in the impregnation method, [6] the ion substitution may take place on the surfaces instead of in the bulk TiO₂ crystallites. In the coprecipitation method, [7] high temperature post heat process may separate out the doping metal ions on the surfaces also. Therefore, to find a method that can well control stoichiometry, desired doping amount is very important.

ZrO₂ doped anatase-type TiO₂ for photocatalytic applications has been studied by several research groups recently. The Ti⁴⁺ ions in an anatase lattice were substituted with Zr⁴⁺ to form Ti_{1-x}Zr_xO₂ solid solution. The doping was fairly effective for the enhancement of the photocatalytic performance when the Zr dopant amount was below 10 at% with UV irradiation. [8-9] Yu et al. reported that ZrO₂ doped titanium solid solution showed enhanced photocatalytic activity from UV light. [8] They explained it by the increase of oxygen vacancy concentration according to the mechanism they proposed. The main reason was that the size difference between titanium and zirconium caused the increase of lattice parameters and cell volume by bring structure defects. Hirano confirmed it with ZrO₂ doped titanium nanoparticles. [9] But, neither of these authors measured the bandgaps of doped materials and the photocatalytic activities with visible light irradiation. Most of these studies were on nanometer-sized particles. There was no report on nanoscale thin films of ZrO₂ doped anatase-type TiO₂ as our knowledge.

Atomic layer deposition (ALD), a thin film deposition technique has attracted more and more attention because of its precise and simple thickness and composition control. It is a surface-controlled process by building the films up single atomic by single atomic layer. The structure and growth of the films are controlled in one reaction sequence involving separated introduction of the precursors and purging. The films produced by this technique are uniform dense, homogeneous and pinhole free. [10]

ALD has been applied for deposition of TiO₂ and ZrO₂ thin films successfully. [11,12] Nitrogen-doped TiO₂ film by ALD was described by Viljami Pore in his paper.[13] The influence of nitrogen doping on the photocatalytic activity of the films in the UV and visible light was evaluated. The films were excited by visible light. But, they suffered from high recombination that caused low photocatalytic activity both under UV and visible light. As our knowledge, there is no other report on doped TiO₂ films by ALD for photocatalytic applications so far. In this work, ZrO₂ doped TiO₂ thin films were deposited by combing the TiO₂ and ZrO₂ ALD processes .The effect of ZrO₂ doping on the structure, composition, surface morphology and photocatalytic activity through the decomposition of stearic acid films were investigated and reported.

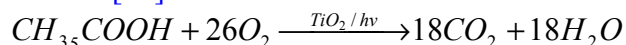
Experimental

All ALD experiments were carried out in a Savannah 100 manufactured by Cambridge Nanotech Inc. Titanium isopropoxide (99.7% from Aldrich), zirconium t-butoxide (99% from Strem Chemicals) and water (from a Barnstead Nanopure Infinity water system) were used as the precursors. All the films were deposited on quartz and p-type silicon wafer (100) at 300°C. The reactor pressure was fixed at 0.1-0.2 torr using nitrogen (Specialty Gases Inc., rated purity of 99.9995%) as a carrier and purging gas. The flow rate of nitrogen gas was set at 15 sccm. The metal precursors were evaporated at 70 °C to ensure enough precursor vapors into the reactor on every pulse. Water was held at room temperature. Pulse times of 0.2s/5s/0.1s/8s were used for metal precursors, N₂, water, N₂, respectively.

Incorporation of zirconium was carried out by depositing TiO₂ and ZrO₂ in an alternating fashion by applying a certain number of titanium oxide cycles followed by one zirconium oxide cycle and then repeating that sequence. Pure TiO₂ and pure ZrO₂ films were produced also for comparison.

Thicknesses of the films were obtained from spectroscopic ellipsometry. Film crystalline structure and crystallographic orientation were examined by using a Rigaku powder X-ray diffractometer and Renishaw's Invia Micro Raman spectroscopy. Film compositions were obtained by Thermo VG Scientific X-ray photoelectron spectroscopy (XPS). Film surface morphology was studied by Zeiss Supra 35VP scanning electron microscope (SEM) The UV-VIS absorption spectra of the films were measured using a spectrophotometer.

The photocatalytic properties of the films were measured by degradation of a solid layer of stearic acid (CH₃(CH₂)₁₆CO₂H, Aldrich, 95%) under visible light source. The TiO₂ -mediated photodecomposition of stearic acid can be summarized as follows:[14]



where $h\nu$ is greater than the bandgap of TiO₂. The absorbance of the asymmetric C-H stretching mode of the CH₂ group at the peak wavenumber 2919cm⁻¹ was monitored by measuring infrared absorption spectrum in transmission mode using a Perkin-Elmer Spectrum FTIR instrument before and after visible light irradiation. A 150-W fluorescent

lamp (Gilway, EKE) with a 390 nm cut-off UV filter (Edmund Optics, NT39-426) was used as the visible light source. The stearic acid layers were dispersed on the TiO_2 sample surfaces by dip-coating method.

Results and Discussion

All the doped and non-doped films deposited were between 100-150nm in thickness. The growth rate was 0.03-0.05nm/cycle, which agrees well with previous reports for TiO_2 and ZrO_2 films with same precursors and deposition temperature.[11,12] Because ZrO_2 has a lower growth rate than TiO_2 , the growth rate of doped films decreased as the relative amount of ZrO_2 pulses increased.

XRD measurements carried out for thin films grown on silicon showed that the pure TiO_2 film had crystalline anatase phase with a (101) orientation (Figure 1). When the Zr/Ti pulse ratio was 9, the anatase structure was retained. As the amount of dopant increased, the anatase phase disappeared. There was no XRD reflection when the Zr/Ti pulse ratio was 5. A non-anatase phase formed at higher zirconium concentrations, which was attributed to the crystalline phase of ZrTiO_4 solid solution. [15]. The positions of these peaks had a small shift as the Zr ratio increased. The pattern of pure ZrO_2 was similar with the report by Kukli, [12] where the broad peak at 35° was addressed to either the (220) reflection of the stable monoclinic phase or the (200) reflection of the metal-stable.

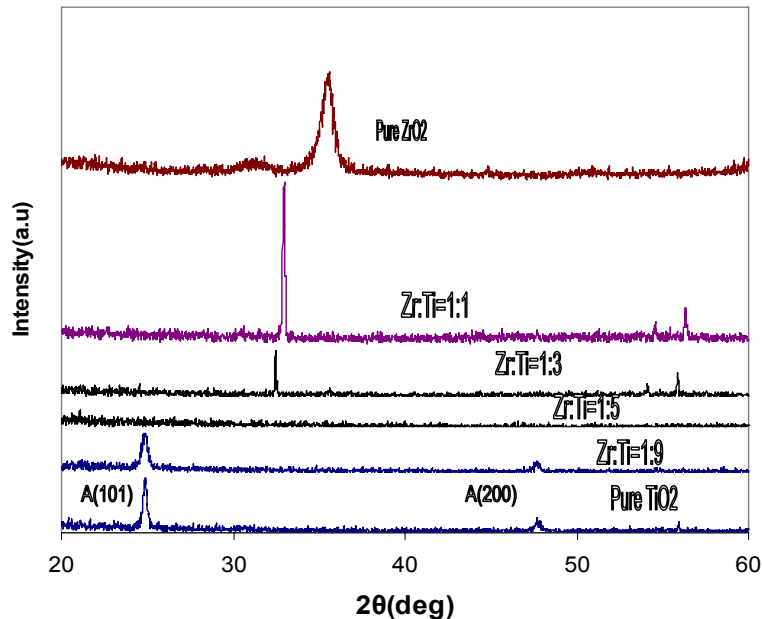


Figure 1: X-ray patterns of deposited films with different pulse ratio grown on Si. “A” means anatase phase of TiO_2

The Raman spectrum of produced films confirmed the XRD results (Figure 2). Only the doped film with 10% Zr pulse ratio and pure TiO_2 showed peaks at $146, 398$ and 637 cm^{-1} which were directly attributable to anatase phase. (Literature values: $143, 396, 516, 639 \text{ cm}^{-1}$) [16]. The literature value of 516 cm^{-1} was believed to be overlapped by strong Si peak at 522 cm^{-1} , which appeared in all the films. There was no additional peak detected which would point to the incorporation of ZrO_2 .

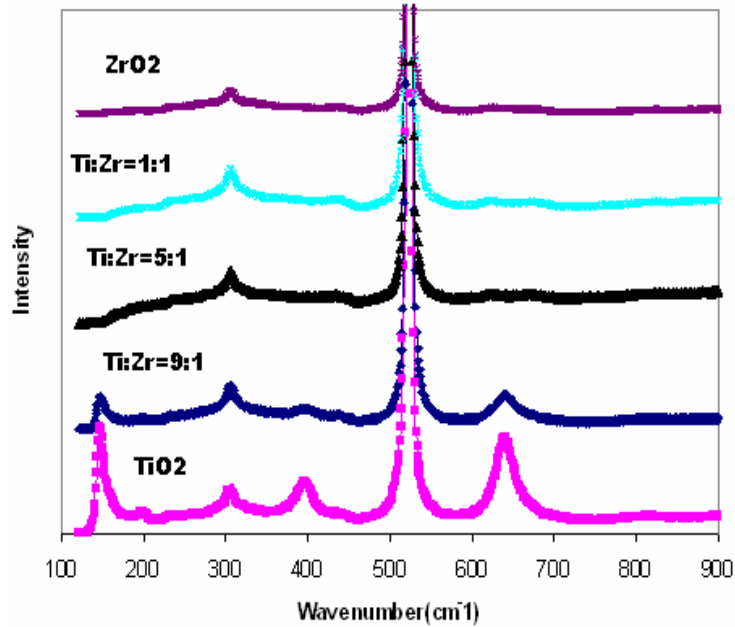


Figure 2: Raman spectra of deposited films with different pulse ratio

SEM images for the surfaces of the doped films are shown in Figure 3. In highly Zr-doped sample (Zr:Ti=5:1), the surface morphology was flat with very low roughness. As indicated in the XRD patterns above, excessive doping of zirconium in the titanium oxide films led to amorphous mixed oxides. When the amount of doped zirconium was low, the surface morphology was as similar as that of pure TiO_2 film, which was composed of nano-crystalline TiO_2 .

Figure 4 shows the XPS spectrum of film with 10%Zr pulse ratio. The corresponding surface composition was determined from the integrated photoemission intensities corrected with appropriate atomic sensitivity factors. Since XPS was performed *ex-situ*, ambient contamination of C was significant. Shown in Figure 5 is the at.% of Zr in each sample with various Zr pulse ratio. Zirconium contents of the films increased roughly linearly as a function of Zr pulse ratio. However, with low Zr pulse ratio, the efficiency of zirconium incorporation into titanium was low also. This must be due to the difference in the reaction kinetics and sub-monolayer deposition rate. Based on these results, we can conclude that the incorporation of Zr into titanium can be achieved by ALD and the Zr doping can be effectively controlled by varying the ration of TiO_2 and ZrO_2 cycles during the deposition. The bonding energy of the main $\text{Ti}2p_{3/2}$ and $\text{Ti}2p_{1/2}$

were 458.5 eV and 463.2 eV, respectively. These values were characteristic of titanium at the oxidation state 4. The Zr 3d photoemission line was observed as a spin-orbit split doublet, (Figure 6) with the oxidized Zr3d_{3/2} at 185.1 eV and Zr3d_{5/2} at 182.1 eV, which indicated that zirconium was fully oxidized as Zr⁴⁺.

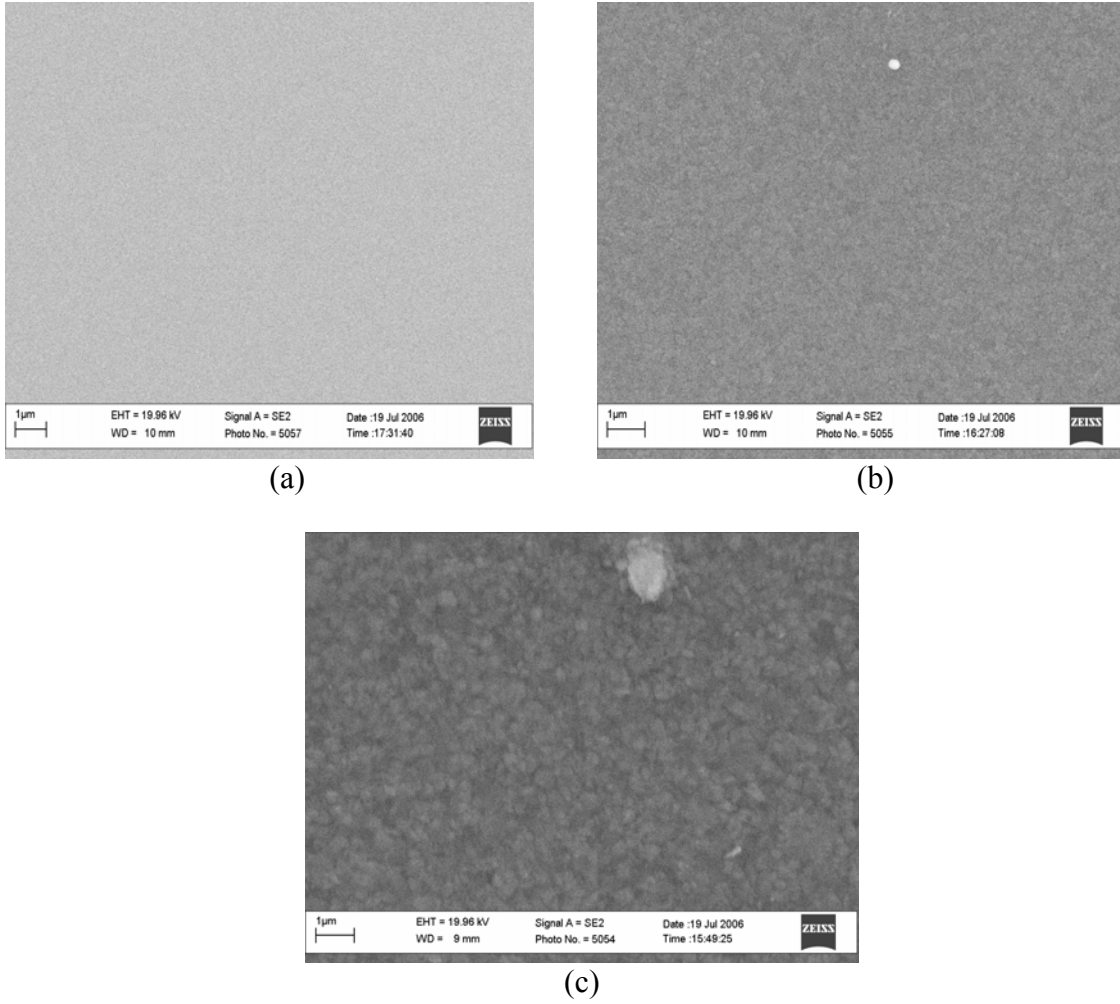


Figure 3: SEM images of the Zr-doped TiO₂ films with different doping ratio: (a) Zr:Ti=1:9, (b) Zr:Ti=1:5, (c) Pure TiO₂

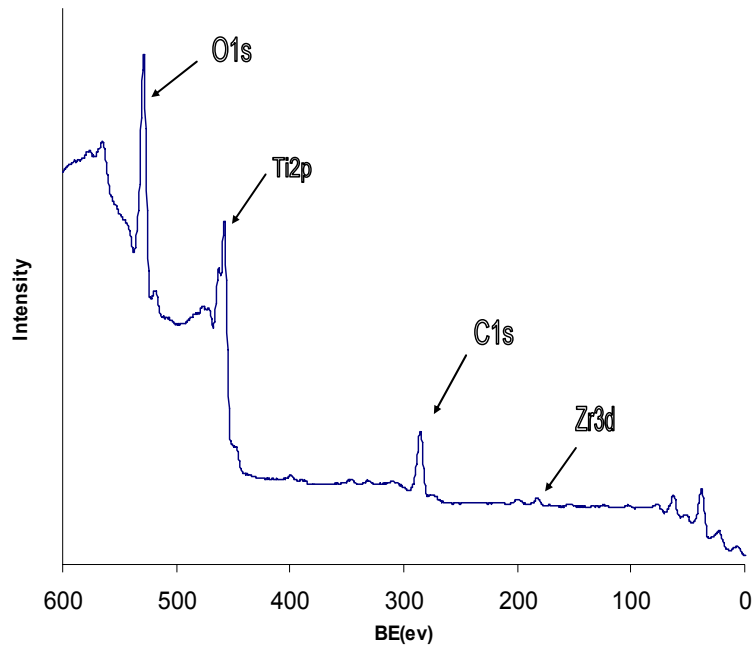


Figure 4: XPS spectrum relative to a Zr-doped TiO₂ film grown on Si (Zr:Ti=1:9)

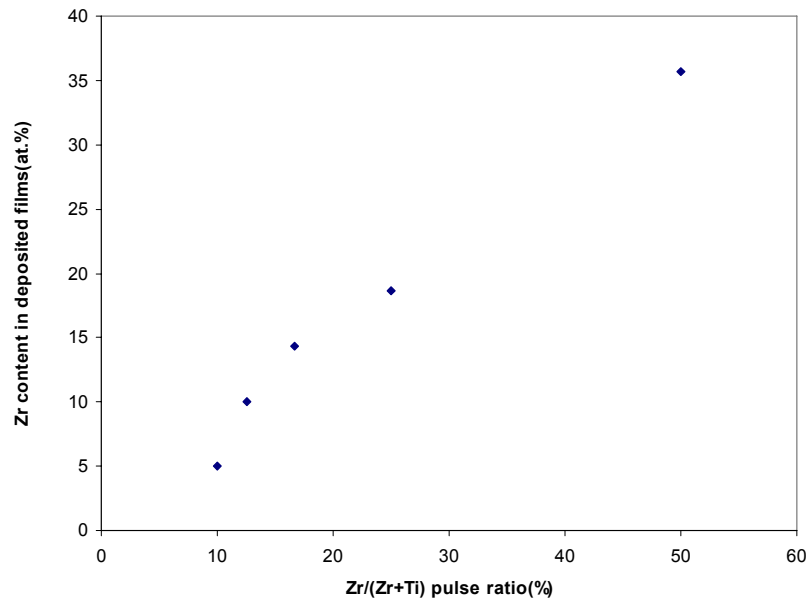


Figure 5: Zr content as a function of Zr to Ti pulsing ratio

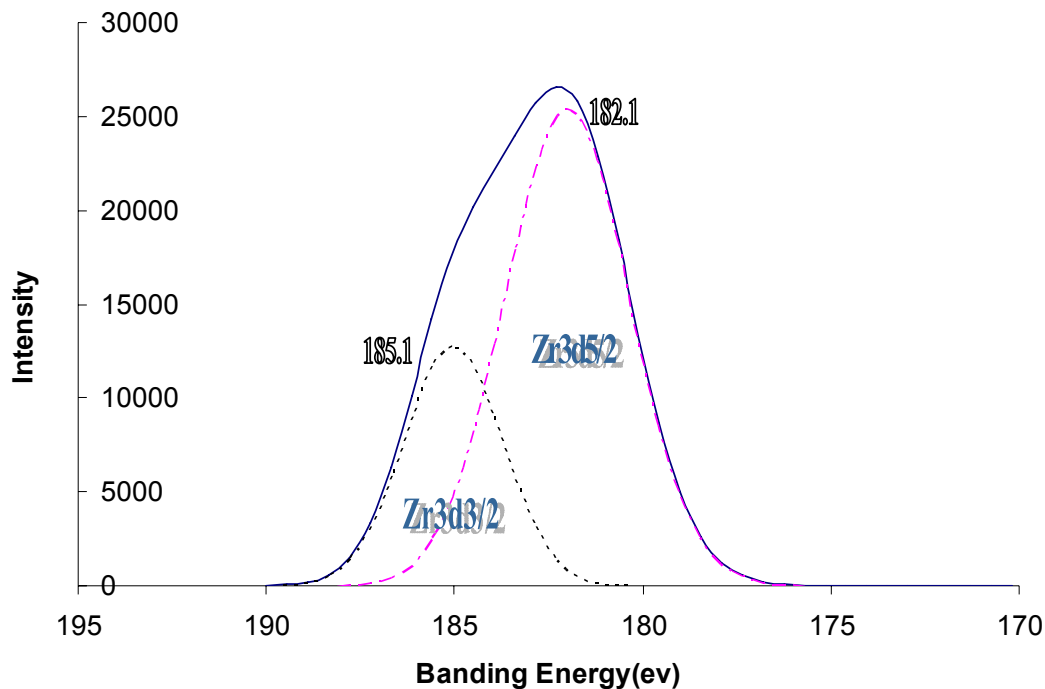


Figure 6: The high resolution Zr3d spectrum

We studied the samples, pure TiO₂ and 10% Zr pulse ratio doped film deposited on quartz which had anatase phase. UV absorption spectra of them are shown in Figure 7. It was significant that the doped film had higher absorption in lower wavelength range (visible light range) than non-doped film. The band gap energies of the two films were estimated by plotting $(\alpha h\nu)^{1/2}$ versus E. [17] The measured band gap of pure TiO₂ was close to the anatase bulk value of 3.2 eV. With the doped film there was a band gap narrowing of roughly 0.2 eV, by this estimation method. It is known that the band gap of ZrO₂ (5eV) is higher than that of anatase TiO₂ (3.2eV). [17] The incorporation of Zr into titanium might bring the isolated impurity state in the band gap and cause the absorption of visible light. Further study is needed to measure the photocatalytic activities with visible light irradiation.

Conclusion

Zirconium doped TiO₂ films by ALD at 300°C retained anatase phase when the Zr doping was below 10%. However, the films were amorphous when zirconium pulse ration increased. The doping amount could be effectively controlled by varying the pulse ratio of metal cycles. The doped film with 10% Zr pulse ratio has great visible light absorption. Further research is needed to optimize the doping amount and to confirm band gap reduction and increased photocatalytic activities.

References

1. K.Honda, A. Fujishima, *Nature* 238, (1972) 37
2. M. Maeda, and T. Watanabe, *J. Electrochem. Soc.*, 153(3) (2006) C186
3. G. Zhao, G. Han, M. Takahashi, T. Yoko, *Thin Solid Films* 410 (2002)14
4. N. N. Negishi, S. Kutsuna, T. Ihara, S. Sugihara, K. Takeuchi, *J. Mol. Catal. A: Chem.* 161 (2000) 205
5. W. Zhang, Y. Li, S. Zhu and F. Wang, *Catalysis Today* 93-95(2004) 589
6. D. Paola, E. G. Lopez, S. Ikeda, G. Marci, B. Ohatani, and L. Palmisano, *Catal. Today.* 75 (2002) 87
7. K. E. Karakitsou, and X .E. Verykios, *J. Phys. Chem.* 97 (1994) 1184
8. J. Yu, J. Lin and R. W.M. Kwok, *J. Phys. Chem. B* 102(1998) 5094
9. M. Hirano, C.Nakahara, K. Ota, O. Tanaike, and M. Inagaki, *J. Solid State Chem.* 170(2003) 39
10. M. Leskela and M. Ritala, *Thin Solid Films* 409 (2002) 138
11. A. Rahtu, and M. Ritala, *Chem. Vap. Depos.* 8 (2002) 21
12. K. Kukli, M. Ritala, and M. Leskela, *Chem. Vap. Depos.* 6 (2000) 297
13. V. Pore, M. Heikkila, M. Ritala, M. Leskela, and S. Areva, *J. Photochem. Photobio. A: Chem.* 177 (2006)68
14. A. Mills, G. Hill, S. Bhopal, I. P.Parkin, and S. A. O'Neill, *J. Photochem. Photobio. A: Chem.* 160 (2003)185
15. A. Rahtu, M. Ritala, and M. Leskela, *Chem. Mater.* 13(2001) 1528
16. Y. H. Chee, R.P. Cooney, R.F. Howe, P.A.W.Van der Heide, *J. Raman Spectrosc.*, 23(1992) 161
17. A. Nozik, *J. Annu. Rev. Phys. Chem.* 29(1978) 189